ABSORPTION RATE STUDIES OF FLEXOGRAPHIC INK INTO POROUS STRUCTURES: relation to dynamic polymer entrapment during preferred pathway imbibition.

P. A. C. Gane
Vice President Research & Development
Paper & Pigment Systems

C. J. Ridgway[1]
Senior Scientist

OMYA, Plüss-Staufer AG
CH-4665 Oftringen
Switzerland

ABSTRACT

The absorption rate of flexographic ink fluids into porous pigmented structures has been measured based on the methods of Gane, Schoelkopf, Spielmann, Matthews and Ridgway (2000). Identification of a preferred network pathway for absorption of low density, low viscosity fluids according to Schoelkopf, Gane, Ridgway and Matthews (2000) allows for correlation to be made between the short-term rate of absorption into a network structure of a coating layer and the observed rate of imbibition into compressed porous block samples of coating pigment. The work extends this correlation from the idealised homogeneity of well-characterised fluids to the removal of a fluid phase formulation, consisting predominantly of water and additives, such as surfactant polymers, from commercial flexographic ink. The ink fluid phase is removed by the absorptive forces of the porous coating network acting against potential surface retardation structures forming at the interface between progressively concentrating ink and the porous medium. The absorption rate of fluid from the ink under supersource conditions is found to be faster than in the case of extracted fluid phase alone. This is interpreted as an obstructing effect of polymers, contained within the extracted fluid phase of the ink, blocking the initial high rate absorbing fine pores. Retention of these polymers in the concentrating ink filtercake acts as an imbibition "pump" keeping the porous structure free from their blocking action. This effect can be incorporated into a modified filtercake model (Xiang and Bousfield 1998) such that, counter to the case of offset inks where a permeability decrease is predicted, the controlling reduced polymer drag found in flexographic ink can be accounted for by developing an effective entrapment factor for the polymer in the ink in terms of a Darcy permeability increase. Analysis using mercury porosimetry on the ink filtercake structure provides information on the proportion of the immobilised ink pore volume fraction which contains the compressible polymer. The solids volume fraction of the filtercake was found to match the sterically stabilised maximum volume fraction for immobilisation.

Keywords: Porosity, polymer absorption, pore modelling, liquid absorption, paper coating, penetration, flexography, printability

[1] Author to whom correspondence should be addressed

INTRODUCTION

Flexographic printing, with its use of environmentally friendly water-based inks is increasing in importance especially for 'point of sale packaging' due to the requirement to create marketing appeal for cartons and boxes. The development of flexography over the years has been described by Moir (1994). High standards of print quality are nowadays expected and, because of this, coated grades of bleached board and unbleached Kraft liner are in increasing demand. For such printing using water-based flexographic inks, rapid drying characteristics are essential, and can be achieved through evaporative loss aided by additives which reduce surface energy and increase fluid phase partial pressure, and by providing strongly absorptive coating layers, which are of particular importance when considering multi-colour formats.

Such absorptive coating layers can be produced using the blocky particle morphology of ground calcium carbonate generally of relatively fine particle size and additional high surface area pigments may be of benefit. To achieve coverage, multi-layer coating is often employed in which the precoat layers can have larger pore size and greater porosity than the subsequent fine topcoat. However, the rate of absorption is not controlled wholly by the absolute level of porosity: the distribution of pore sizes in the coating structure network is equally important especially when considering the rate of absorption. The importance of preferred pathway absorption has been described by Schoelkopf et al. (2000). There is a need for the high capillarity developed in the finer pores in order to ensure rapid absorption during the short times in which the ink is in contact with the coating layer during high-speed printing processes to avoid blocking, i.e. marking of adjacent surfaces. This high capillarity is required in particular to overcome the additional drag which is created by the partially deposited ink layer, which has been proposed effectively to form a filtercake as it is progressively dewatered. Xiang and Bousfield (1998) have put forward a model for the formation of such filtercakes and, primarily in relation to the offset printing process, their retardational drag effects. For optimal absorption properties it is necessary to consider the force balance between the capillary absorption into the network and the permeability characteristics of the filtercake, rather than simply strive for ever greater porosity.

It was therefore decided to investigate the absorption of the fluid phase of a flexographic ink[2], free of pigment particles, into model porous structures and to compare it with the absorption rate from the whole ink in order to study the significance of the potential effect of the formed filtercake and to determine if such a model is indeed representative of the processes involved. As we shall describe below, counter to the expected retardational effect of the forming ink filtercake, the ink structure was found to act as an effective imbibition pump increasing the rate of absorption of fluid from the ink above that seen for the fluid phase alone. The reduced rate of absorption of the fluid phase alone is interpreted as an absorption and/or adsorption of dispersed polymer thereby forming a blockage of the surface pores of the substrate medium. We have modified the model of Xiang and Bousfield (1998) to describe the dynamic entrapment of polymer within the forming filtercake which then acts to reduce

[2] Rot VSW 230, a product of Printcolor Gravoflex AG, CH-4800 Zofingen, Switzerland.

the blocking of the surface pores of the substrate, and used the model to form an expression for the Darcy permeability increase afforded by the capture of the polymer. This additional factor in the case of flexographic inks is seen as a major departure from the accepted models for other printing methods.

Further analysis using mercury porosimetry on the ink filtercake structure provides information on the proportion of the immobilised ink pore volume fraction which contains the compressible polymer. It is hoped that these extended evaluations will be of assistance in the design of coatings which will have enhanced absorptivity in a wide range of water-based printing and coating applications.

DEFINING THE FLEXOGRAPHIC INK

Flexographic inks have been developed for use on a wide range of substrates, these include non-absorbent films and highly absorbent heavy weight coated packaging grades. The rheological behaviour of low-viscosity, water-reducible flexographic printing inks has been investigated by Havlinova et al (1999). They conclude that the inks exhibit pseudoplastic flow behaviour. The ink drying characteristics are achieved by a combination of rapid evaporation of the water-based fluid phase together with some absorption where possible into a coating structure. The increasing diversity of print formats required for sophisticated aesthetically pleasing customer impression demands the design of complex multi-colour formats. Trends are emerging in which the control of the balance between feathering, fill-in and mechanical pin-holing means that increasingly reduced inks are being used (Finley 1997). This places greater demands on the designed absorbency of coated substrates.

The multi-phase system constituting a flexographic ink is separable into a liquid phase and a solids-containing structural phase. The fluid phase obtained by centrifugation has been shown to contain film forming polymers which are identical to those contained in virgin reducer (the fluid diluent used in flexographic printing to reduce the viscosity of the ink), as shown in the comparison of Fourier Transform Infrared Spectra taken from the dried centrifuged fluid (mobile) phase and dried reducer respectively, Figure 1, the samples being dried at 110 ^{o}C.

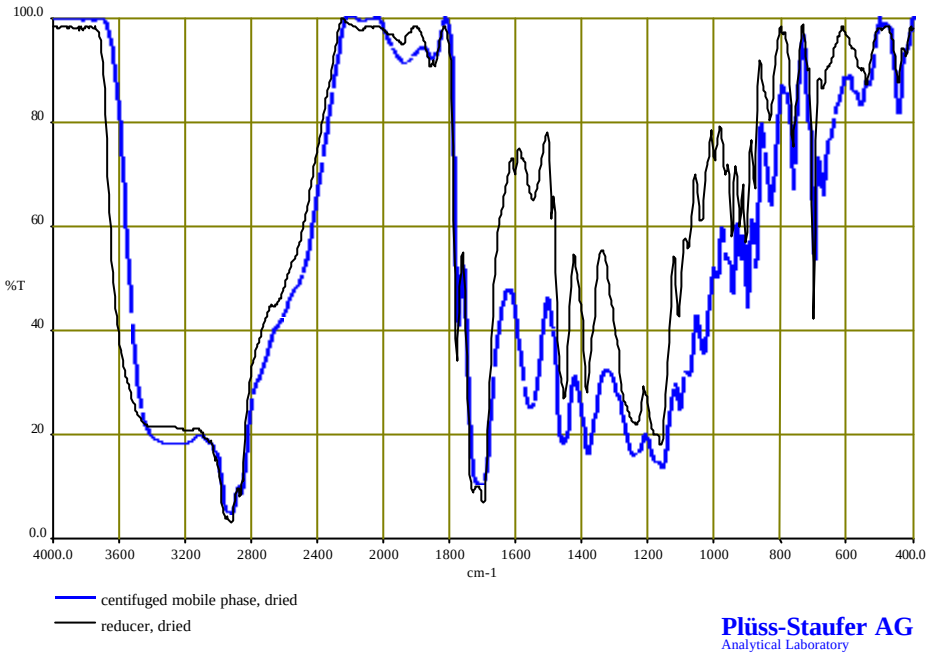

Figure 1. FTIR spectra of centrifuged fluid phase and reducer

The spectra were run over a wave-number range from 400 to 4 000 cm^{-1} in transmission mode using a silver chloride carrier. Characteristic absorptions were seen for such substances as styreneacrylate and resin. There were also absorptions indicating alkyl ketone dimers together with some bands in the centrifuged fluid phase due to incomplete removal of what was assumed to be organic pigment. Other absorptions were assignable to a range of compounds including glycols, esters, alcohols, fatty acids and salts.

The viscosity of the centrifuged fluid phase was shown to be a constant at constant shear stress independently of time, Figure 2. Any effect arising from dissolved polymer was therefore assumed to be small at least at the initiation of concentration, i.e. at the starting solution concentration, and a characteristic viscosity was therefore assumed.

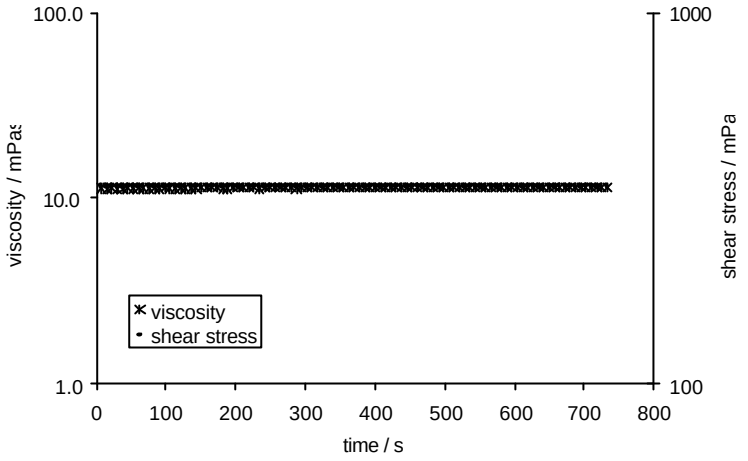

Figure 2. Viscosity at constant shear rate of centrifuged fluid phase

In contrast, the whole ink was shown to be slowly shear thinning under relatively low shear rate conditions (30 s^{-1}), as shown in Figure 3a, with an elastic and viscous recovery, Figure 3b, after cessation of further shearing for one minute at 360 s^{-1}, using a constant stress[3] of 0.48 Pa under oscillation of 0.5 Hz at room temperature.

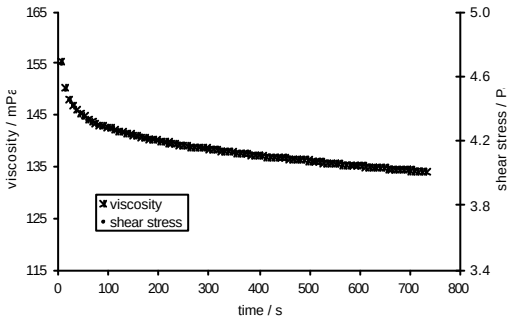

Figure 3a. Shear thinning of whole ink

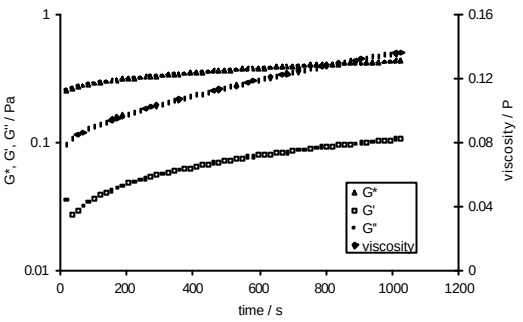

Figure 3b. Elastic and viscous recovery of whole ink

A characteristic recovery time, t_0 ~ 550 s, for the ink was approximated by considering a single exponential of the form

$$h(t) = \left(h(\infty) - h(0)\right)\left(1 - e^{-t/t_0}\right) + h(0) \qquad \text{Eqn (1)}$$

where $h(0)$, the sheared viscosity at 360 s^{-1}, was taken to be 0.078 Pas. A comparison between the model recovery and the observed data is shown in Figure 4.

[3] rheological measurements were made using a StressTech rheometer – a product name of ReoLogica Instruments AB, Lund, Sweden

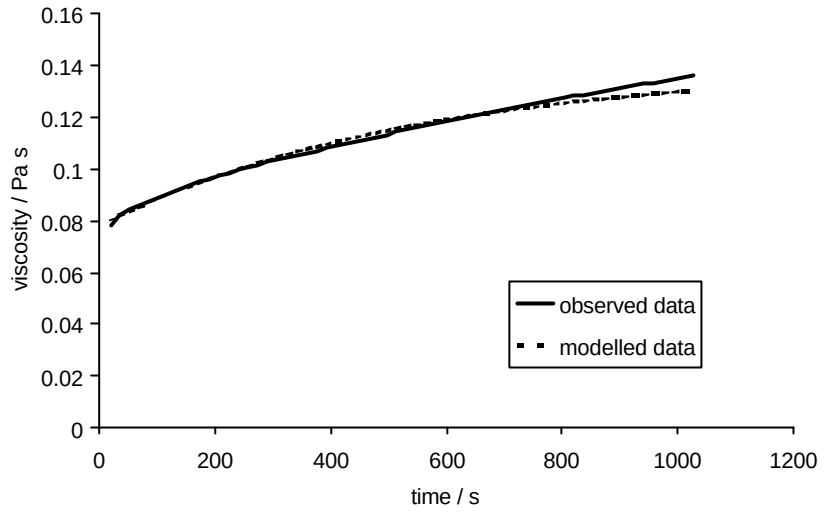

Figure 4. Model viscosity recovery and observed data for the whole ink

This recovery time is long compared to the setting requirements on a press and is a clear indication that ink levelling and eventual setting is not rheologically related at the initial ink concentration but dependent on increasing concentration and associated meniscus forces. This is in stark contrast to the recovery and levelling processes in off-set printing proposed by Desjumaux et al (1998). The slow shear thinning behaviour will, however, tend to influence the absorption behaviour of fluid from the ink as the establishment of flow through the tortuous interface between ink and substrate will create shear thinning of the ink as a function of time. If this is related to polymer-polymer interactions or interactions between those polymers and the other components of the ink, it will act to assist absorption until a steady state is reached after $t_0 \sim 550$ s. We shall see later that this timescale closely represents the time needed to establish absorption rate equilibrium between the fluid phase alone and the whole ink.

The remaining solid phase components in the ink tested were shown to be mixtures of inorganic (pigment) and organic species (waxes, dispersants etc.). The latter were shown to exist also in the standard extender fluid supplied to accompany this ink, i.e. the fluid additive provided to extend the colour component whilst maintaining ink viscosity. The extender separated clearly into two phases. The FTIR traces of the less dense organic phase and the remaining polymer solution are compared in Figure 5.

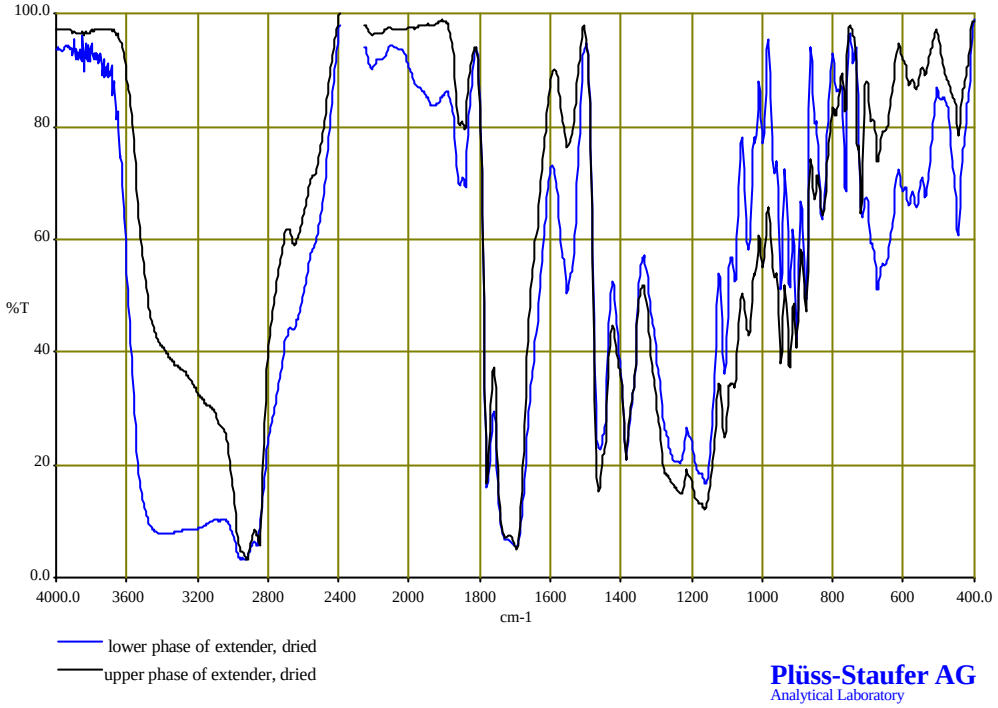

Figure 5. FTIR traces from the two phases of standard extender fluid

It can be seen that the two phases differ primarily only in terms of the water content, indicating that the polymers involved have either an enormously broad molecular weight distribution, ranging from macro polymerisation down to dissolved micro species, or that polymer precipitation and/or souring (precipitation of nitrocellulose) had occurred. Therefore, to simplify the experimental structure, absorption studies were made only using whole ink, centrifuged fluid phase from the whole ink (same as reducer) and pure water to elucidate the primary separation mechanisms occurring at the ink coating interface.

Surface tension, component densities and polymer concentration

Surface tension of the centrifuged fluid phase was measured using a Krüss Digital Tensiometer K10T with a ring configuration. The density of the centrifuged fluid phase and the whole ink were calculated by weighing a known volume of fluid in a predetermined vessel. The density of the solid phase of the ink was determined after drying the ink in a thermobalance at 150 ^{o}C, subsequently ground, and its density determined using a pycnometer. The polymer content of the centrifuged mobile phase was determined using a thermobalance at 150 ^{o}C.

Contact angle

The static contact angle of the mobile phase was measured on a surface of a pure calcium carbonate crystal, which had been wet ground using the same dispersing agent as for the absorption and porosimetry samples. The contact angle q was found to be 16.25^{o}. The microroughness of the surface was measured with a confocal laser scanning microscope (Lasertec 1LM21). The microscope scanned

perpendicular to the surface at 4 780 points with a spacing of 0.38 μm, and measured a variance of 0.37 μm^2. Derivation of the experimental contact angle is illustrated by the schematic in Figure 6, and determined by

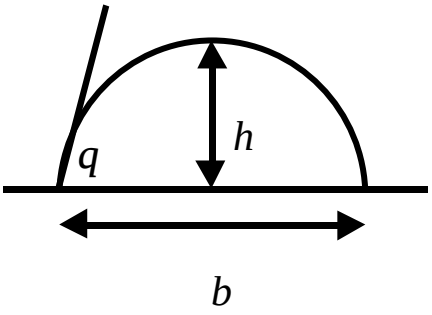

Figure 6 Schematic diagram for static contact angle measurement

$$\frac{1}{2}\tan\left(\frac{q}{2}\right) = \frac{h}{b} \qquad \text{Eqn (2)}$$

where h is the height of the drop, b is the base length and q is the contact angle. This is expected to represent the liquid-solid interactions within the porous network of a typical ground calcium carbonate coating.

An overview of the ink constituent properties is shown in Table 1 below.

Table 1.

	Density / kgm^{-3}	Viscosity / $kgm^{-1}s^{-1}$	Surface tension / Nm^{-1}	Contact angle for fluid on dispersed calcite / ^{o}	Polymer concentration / %
Centrifuged fluid phase	1035	0.0113	0.0338	16.65	26.27
Whole Ink	1120			27.28	
Solid phase	1778				

EXPERIMENTAL

Absorption into a porous medium

To observe and quantify the absorption characteristics of a compacted pigmented coating we adopted the methodology described by Schoelkopf et al. (2000) in which a ground calcium carbonate, which is commonly used as a main component in board coatings, derived from a polyacrylate dispersed wet

ground limestone (Omya Hydrocarb OG) with a particle size characteristic of 60 % by weight of the particles less than 2 μm in diameter, was spray dried and compacted in a steel die at 259.4 ± 2.7 MPa. The grain size before compaction, and the compaction pressure itself, could be carefully controlled to give a reproducible and relatively homogeneous porous structure. Such homogeneity was required so that similar specimens could be used for the fluid absorption and mercury porosimetry experiments for further void space characterisation. The sample was consolidated, and therefore did not require a sample vessel for the fluid absorption experiments, thus eliminating uncertainties of fluid interactions with such a vessel.

Part of the sample was studied by mercury porosimetry to determine its percolation. The rest of the compact was cut and ground to form several 12 mm cubic blocks, using a rotary disc grinder and a specially constructed, precisely adjustable jig.

To reduce artefacts caused by the wetting of their outer surfaces, samples were coated with a thin barrier line of silicone around the base of the vertical edges arising from the basal plane. The remainder of the outer planes were not coated, to allow for the free movement of displaced air during liquid absorption, and to minimise any interaction between the silicone and the absorbed liquid.

Wetting apparatus

The rate of liquid uptake was measured using an automated microbalance, namely a PC-linked Mettler Toledo AT460 balance with a precision of 0.1 mg, capable of 2.7 measurements per second. To provide a sufficiently slow and precise approach of the sample down to the liquid surface, a special sample holder was constructed according to Gane et al (2000), Figure 7. The chamber around the balance base plate enabled a controlled atmosphere to be established, shielded from external air and humidity. The walls of the chamber included an array of gutters which could be filled with silica gel for working with hygroscopic liquids, or with the liquid itself to allow the establishment of a saturated vapour. Additionally, there was a gas inlet, which could be used to keep the cell under a steady stream of an inert gas such as nitrogen.

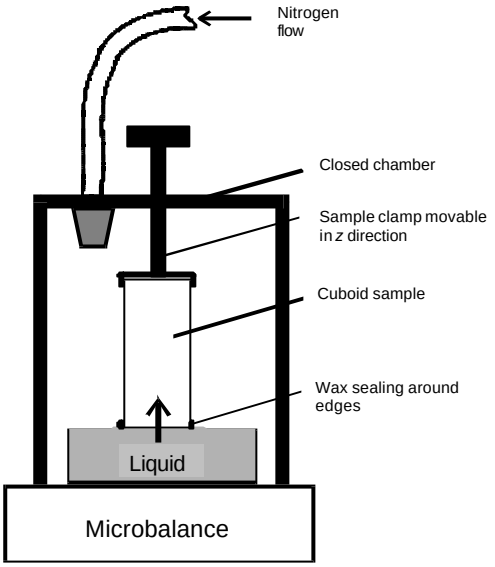

Figure 7 Absorption apparatus, Gane et al. 2000a

All apparatus, gases and samples in this study were maintained at 23.0 ±1.5°C. Prior to the absorption experiments, each porous block sample was placed in a 5 litre chamber. The chamber was then flushed through with dry nitrogen, and the sample left to equilibrate for 48 hours. The absorption experiments themselves were performed in the balance chamber described above, which was flushed with a steady stream of dry nitrogen flowing at 1 litre min^{-1} . The evaporation rates of the fluid phases from the supersource reservoir were measured so the absorption data could be corrected for this apparent weight difference.

Using this technique the micro-scale absorption characteristics of thin structures could be scaled to observably realistic volumes under supersource conditions.

Mercury porosimetry

A Micromeritics Autopore III mercury porosimeter was used to measure the percolation characteristics of the samples. The maximum applied pressure of mercury was 414 MPa (60 000 psia), equivalent to a Laplace throat diameter of 0.004 µm. The equilibration time at each of the increasing applied pressures of mercury was set to 60 seconds. Using the method of Gane et al (1995) the mercury intrusion data were corrected for mercury compression and penetrometer expansion. A further correction was then made to correct for the compression of the solid phase of the sample. These corrections are illustrated in Figure 8 giving a porosity of 27.1 % and bulk modulus of 0.06 GPa.

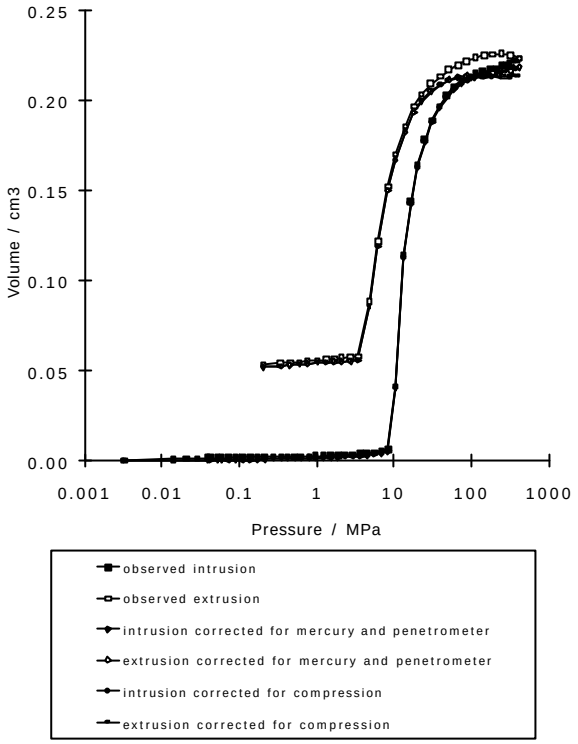

Figure 8 Pore-Comp corrections for percolation of the porous block sample

Absorption results

Figure 9 shows the absorption of the centrifuged fluid phase and as absorbed from the whole ink into the sample block expressed in terms of the mass loss per unit area, as a function of time, from the fluid supersource corrected for evaporation. To minimise the effect of increased evaporative surface area the absorption data were terminated when the absorption length exceeded the depth of the silicone ring at the base of the sample.

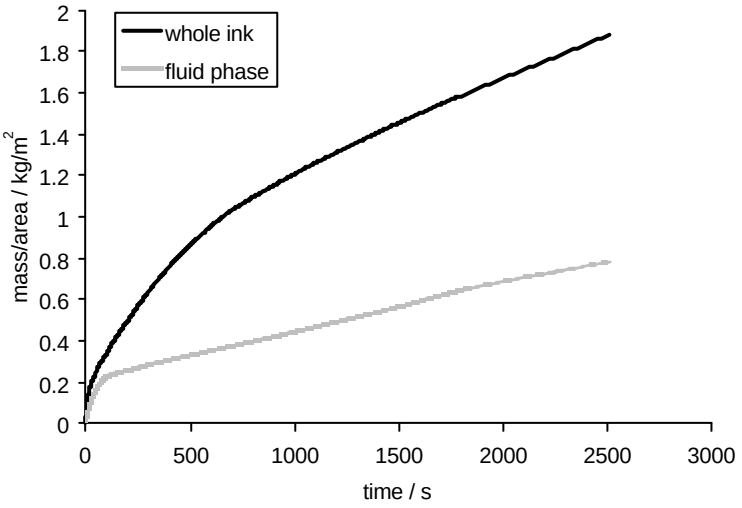

Figure 9 Absorption of whole ink and centrifuged fluid phase as a function of time

The curve for the whole ink lies above that for the centrifuged fluid phase. This is at first partly attributed to the formation of an immobilised layer, or wet filtercake, on the base of the block effectively removing more weight from the supersource than actually would represent the amount of fluid phase that has been absorbed into the block, assuming that any contribution from buoyancy is negligible, i.e. fluid phase included in the wet filtercake is effectively independent of the more dilute ink in the remaining supersource. This is justified by assuming that the capillary flow restriction within the finely forming immobilised layer is greater than the energy loss of the viscous flow of the ink. As we shall see later, it is secondly attributable to an additional factor related to the polymer blocking of pores in the substrate.

Corrections for the mass build-up of filtercake were made by repeating the experiment a number of times, each time terminating the absorption at a chosen time interval and determining independently the mass of the immobilised layer. To improve the statistics of thickness estimation the experiment duration was extended ignoring the evaporative loss limit applied above as this was assumed to have no impact on the submerged filtercake. The characterisation of the filtercake is described in the following section.

Characterising the immobilisation

To determine the wet filtercake weight, the block was removed from the apparatus and weighed. At this stage it was assumed that there was a solid filtercake adhering to the block and a layer of wet ink forming a fluid boundary adhering to the filtercake. The block was dabbed onto a non-absorbent glass surface and reweighed. It was assumed (and later checked by repeated dabbing) that the wet ink layer divided itself equally between the glass surface and the filtercake following the expected 50:50 film split ratio for a fluid in contact with two perfectly smooth non-absorbent surfaces. It is assumed that the filtercake conforms to this boundary condition at this stage, as it is still a saturated microstructure. This allowed the weight of the block plus the wet filtercake plus the absorbed fluid phase to be determined following the schematic in Figure 10 and described as follows:

1. The block, with its absorbed fluid and associated filtercake and fluid phase within the cake, is weighed and allowed to dry under room conditions. It is assumed that all the evaporative components of the fluid phase are lost from both the block and the filtercake during this drying process.
2. Reweighing the block after drying and subtracting the initial weight of the unwetted sample block then gives the dry filtercake weight.
3. To convert this to the wet filtercake weight the porosity of the dry cake is measured independently by mercury porosimetry (see below), and the additional weight of fluid phase needed to fill this voidage is then calculated. The weight of the wet filtercake thus determined is then subtracted from the weight loss from the supersource to give the weight of absorbed fluid phase.
4. It is possible to use the data derived above in a further step by taking the wetted block with its associated fluid phase content and adherent filtercake and subtracting the wet filtercake weight and

the dry block weight to give the weight of the fluid phase absorbed. This can be compared to the absorption data from the supersource experiment and is shown in Figure 11. This comparison gives a rate of evaporative loss from the sample block throughout the time period of the handling and could be interpreted to represent the loss expected under non-saturated vapour conditions.

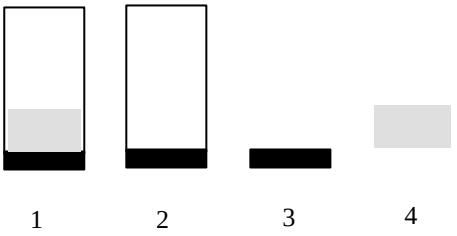

Figure 10 Schematic showing the stages of weighing to determine the actual weight of fluid uptake

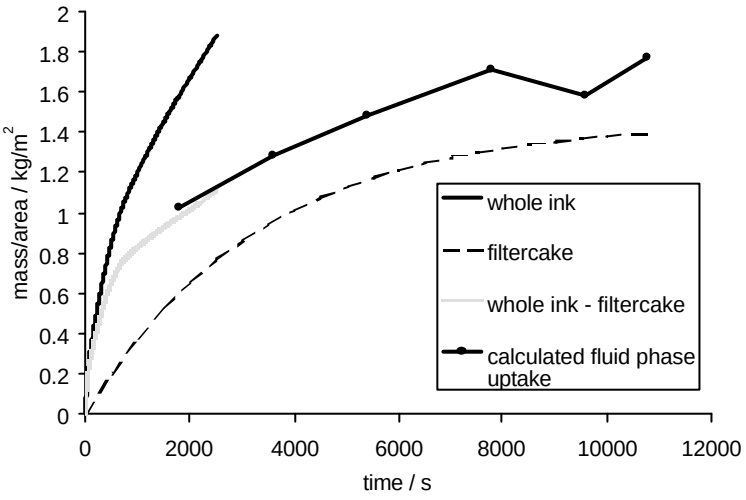

Figure 11 Calculated fluid phase uptake in mass per unit area of sample cross-section

As we see by comparing Figure 9 and Figure 11 the uptake rate is still greater for the ink than for the fluid phase alone even after the applied weight correction for the filtercake. This difference is therefore attributed to the effect of dissolved polymer and its distribution between the ink filtercake and the surface pores of the absorbing substrate discussed in the following sections.

The role of dissolved polymer

Further experimentation was made to establish the action of dissolved polymer in the fluid phase in respect to the absorption dynamics. Depending on the rate and absolute level of concentration the deposition, adsorption or precipitation of polymer can occur either within the filtercake or within the porous absorbing structure or both. For example, the effect of surfactant on the absorption rate of water into a porous structure is well documented and is retarded compared with simple wetting fluids

due to the dependence of the wetting front progress on the diffusion of the polymer. Furthermore, size exclusion of polymer from the porous structure would lead to blanking off of entry pores effecting a further contribution to drag. This extra drag contribution is clearly shown in Figure 12 where the absorption dynamics for the fluid phase are compared with that of pure water.

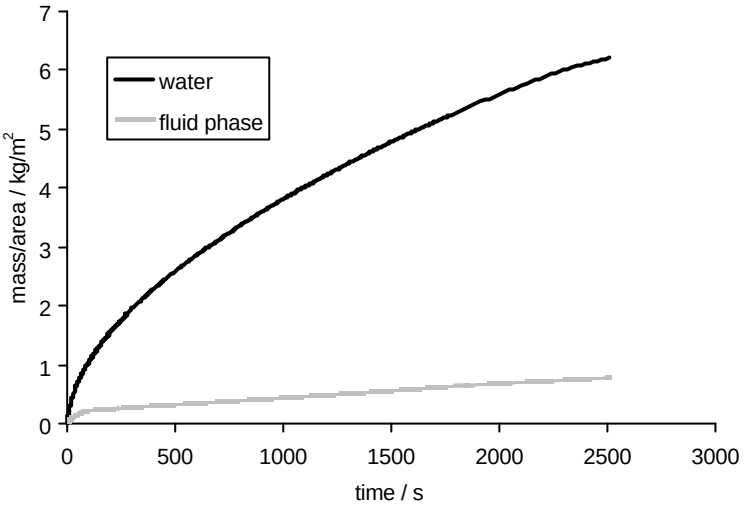

Figure 12 Absorption of ink fluid phase compared with pure water

Deposition of polymer within the entry pores of the block was also confirmed by removing the dried filtercake in step 3 above and comparing the remaining weight of dried sample block with the original unwetted sample block weight. The difference is a measure of polymer absorbed into or adsorbed onto the sample block.

Table 2

Experimental duration / s	Dry block before experiment / g	Block dried after experimentation / g	Difference in dry block weights / g	Mass of ink fluid absorption after wet filtercake correction / g	Polymer concentration in absorbed fluid / %
1800	4.2955	4.3272	0.0317	0.1009	23.9
3600	5.0701	5.1173	0.0472	0.1312	26.5
5400	6.3833	6.4450	0.0617	0.1772	25.8
7800	5.1539	5.2262	0.0723	0.2532	22.2
9600	4.6868	4.7622	0.0754	0.3115	19.5
10800	4.6714	4.7517	0.0803	0.3539	18.5

As we see from Table 2 above, initially ($t > 1\ 800$ s) the polymer concentration moving with the fluid phase into the porous medium equals that of the polymer concentration found in the centrifuged free

fluid phase (26.27 %). This indicates that polymer begins to be transported into the coating structure during the absorption, Figure 13a. The polymer concentration in the absorbed fluid then slowly falls off indicating a deposition of polymer within the surface structure of the sample block. If we look at the schematic diagram in Figure 13b we see that the meniscus front of the fluid phase as it absorbs into the sample block becomes curved with minima at the corner edges of the block. This is in contrast to the planar meniscus generally observed for pure fluids and indicates the effective concentration of polymer blanking as a function of external surface area. The implications for anchoring of ink into the surface micro-structure of the coating will relate to the ratio of absorbed to retained polymer distributed between the coating and the consolidating ink.

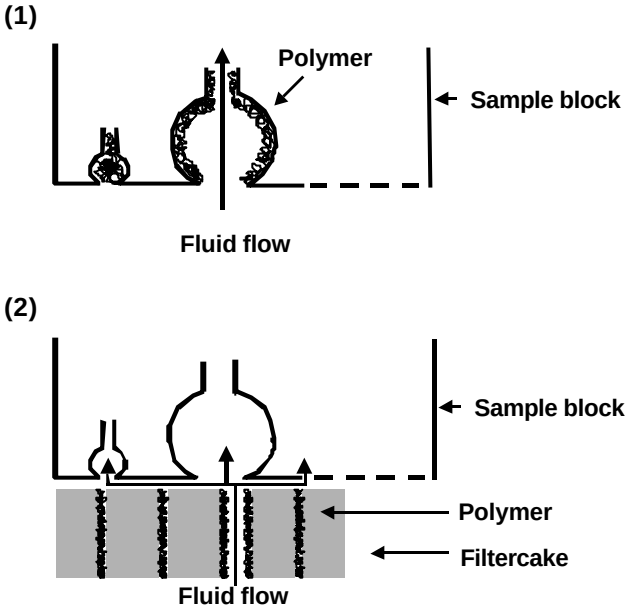

Figure 13a Polymer blanking for: (1) Fluid phase (2) Polymer captured within filtercake at the initial stage of absorption

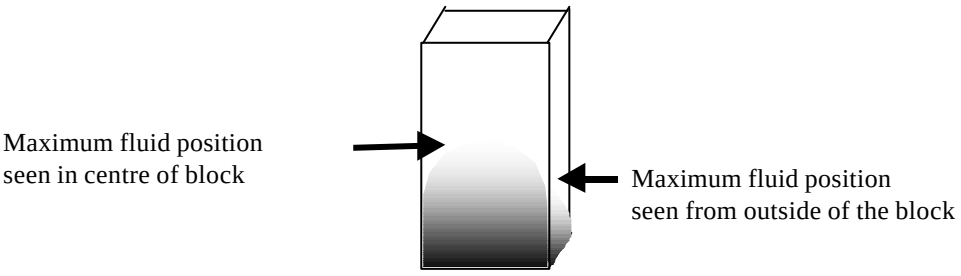

Figure 13b Meniscus front of absorbed flexographic ink fluid as it progresses into the block

Characterising the filtercake structure

We see that the retention of polymer by the filtercake allows a somewhat faster absorption of fluid from the ink than when compared to the fluid alone. To model these effects arising from the porous filtercake it is necessary to characterise the void space within it. Two forms of consolidated ink were studied, the first as dried pre-formed filtercake, i.e. as removed from the sample block after absorption for a given time, and, secondly, ink dried under vacuum (50 mbar). Mercury porosimetry was used to probe the intrudable volume within these two structures. Weight differences were also noted and shown to correlate with the polymer loss from the filtercake during absorption identified above.

Application of the compression correction (Gane et al. 1995) shows the large effect due to the elastic deformation of the retained polymer content on both the filtercake and the dried whole ink, Figure 14a and 14b respectively. Only in the case of the filtercake was there any inelastically intrudable porosity, i.e. pores unfilled by polymer.

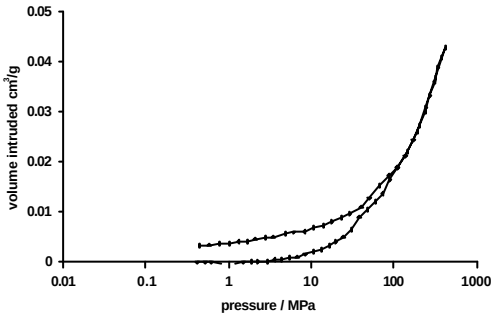

Figure 14a Mercury porosimetry data for filtercake

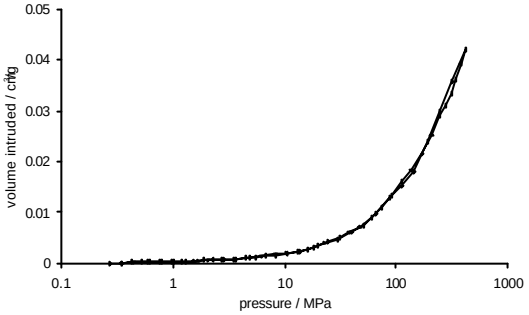

Figure 14b Mercury porosimetry for whole ink

This genuine open voidage in the filtercake was shown to be as low as 0.44 % and clearly not representative of the percolation characteristics of the wet filtercake. Therefore, it is envisaged that the acting pore volume controlling percolation under wet conditions matches the porosity of both the unfilled and polymer filled void structure of the dried samples while the polymer remains solved in the wet state. The total porosity of the filtercake could therefore be determined by including the elastically deformed intrusion volume and was found to be 6.3 %. In the case of the ink the percolation can only be derived from totally polymer filled voids giving a value in turn also of 6.3 %. Since these values are effectively equal we can conclude that there is little or no shrinkage difference between dried filtercake and dried ink. Using the porosity thus determined, the weight of wet filtercake adhering to the sample block is calculated by including the density of the mobile phase occupying the assumed voidage.

We now obtain the skeletal densities for the filtercake and ink from the porosimetric intrusion as 1.7 gcm^{-3} and 1.6 gcm^{-3}, respectively. We can also conclude that the density contribution of dissolvable polymer is small by noting that by independent non-intruding pycnometry, the derived skeletal density of the filtercake is within comparative experimental error equivalent to that of mercury intrusion porosimetry. For example, for dried ink the difference would be expected to be larger than for dried

filtercake, due to the lack of imbibing voidage in the dried ink, with the porosimetry value being logically larger; however, the pycnometer records a consistent value of 1.8 gcm^{-3}.

The volume fractions of wet filtercake and of whole ink were therefore found by combining the relevant skeletal densities and sample weights to obtain ϕ_f (= 0.77) and ϕ_i (= 0.07). The determined value of 0.77 for the volume fraction of the filtercake is exceedingly close to the theoretical maximum of 0.768 for the colloidal packing of Brownian spheres (Frith et al. 1990) under conditions of polymer (steric) repulsion. This suggests that the stabilisation of the ink pigment is effectively steric rather than electrostatic (Macosko 1994).

The absorption characteristic of the dried filtercake was studied by re-immersion into centrifuged fluid phase. The reabsorbed fluid volume amounted to 20 % of the filtercake volume which is higher than the *non* elastically intruded mercury. This indicates that the fluid absorption into the filtercake proceeds through a combination of void filling and inter-polymer diffusion achieving a near complete filling of the assumed fluid phase volume fraction held within the original wet filtercake (1- ϕ_f).

Modelling the absorption

The force difference between the absorbing sample block and the filtercake can be expressed as:

$$\Delta P(t) = \Delta P_{\text{block}}(t) - \Delta P_{\text{filtercake}}(t) \qquad \text{Eqn (3)}$$

where $\Delta P_{\text{block}}(t)$ is the effective driving pressure associated with free fluid phase imbibition into the porous medium and $-\Delta P_{\text{filtercake}}(t)$ would be the pressure drop across the filtercake if it were retarding, both determined at time t. The same expression can be used even in the case here where the filtercake capture of otherwise pore-blocking polymer leads to a recorded positive or pumping pressure action. Both $\Delta P(t)$ and $\Delta P_{\text{block}}(t)$ are experimentally derivable from the observed absorption curves for the whole ink and the centrifuged fluid phase respectively. Since we have shown that some polymer deposition occurs progressively in the absorbing structure we maintain $\Delta P_{\text{block}}(t)$ as a varying function with time rather than relating it through volume uptake to a simple Hagen-Poiseuille drag based on constant pore dimensions as is done by Xiang and Bousfield (1998) in their model for offset inks.

Associated with each absorption curve is an equivalent hydraulic radius which in this case, once again due to the polymer deposition, is also varying as a function of time. For a polymer-free absorption, the hydraulic radius for the fluid phase alone entering the block would be experimentally constant. The two hydraulic radii, $R_{\text{ink}}(t)$ and $R_{\text{fluid}}(t)$, are obtained by differentiating the respective plots of Darcy imbibition length $L(t)$ against $\sqrt{t}$, where the porous substrate has a porosity $\boldsymbol{f}$, and in the case of the ink after the experimental correction for filtercake weight, where

$$L(t) = \frac{V(t)\boldsymbol{f}}{A} \quad . \qquad \text{Eqn (4)}$$

Using the definition of hydraulic radius in the viscous regime of Lucas-Washburn

$$\frac{\mathrm{d}L^2(t)}{\mathrm{d}t} = \frac{R(t)g\cos\theta}{2\eta} \qquad \text{Eqn (5)}$$

where η is the experimentally determined viscosity of the centrifuged fluid phase. $R_{\mathrm{ink}}(t)$ and $R_{\mathrm{fluid}}(t)$ are shown in Figure 15, for the whole ink and centrifuged fluid phase respectively.

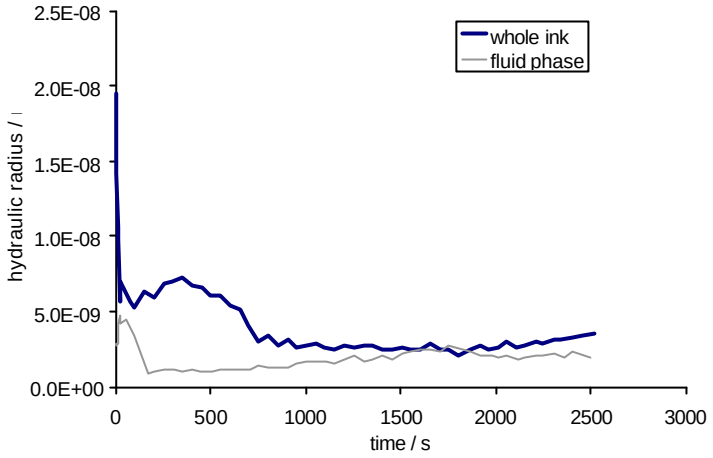

Figure 15 $R_{\mathrm{ink}}(t)$ and $R_{\mathrm{fluid}}(t)$ for centrifuged fluid phase and whole ink

Adopting the Laplace meniscus pressure within the hydraulic radii

$$\Delta P(t) = \frac{2g\cos\theta}{R(t)} \qquad \text{Eqn (6)}$$

we obtain the respective values for the driving pressure and the total pressure for inclusion in equation 3, from which experimental values for $\Delta P_{\mathrm{filtercake}}(t)$ can be determined.

The flow through the filtercake is controlled by Darcy's law as

$$\frac{\mathrm{d}V(t)}{\mathrm{d}t} = \frac{K(t)\Delta P_{\mathrm{filtercake}}(t)}{\eta\, l(t)} \qquad \text{Eqn (7)}$$

where $\mathrm{d}V(t)/\mathrm{d}t$ is the volume rate per unit area passing through the filtercake absorbing into the sample block. $K(t)$, in the case of a viscous drag, is the Darcy constant ($K \rightarrow \infty$ represents no resistance and $K \rightarrow 0$ complete blocking of the flow) and $l(t)$ is the filtercake thickness. We use the same expression but now interpret $K(t)$ as a drag *reduction* or pump compared with the polymer blocking caused by fluid phase alone, such that increasing $K(t)$ indicates a strong pumping action or capture of polymer within the filtercake aiding the absorption process by keeping the absorbing pores of the substrate free from polymer.

The filtercake thickness $l(t)$, shown in Figure 16, is obtained experimentally using the above determined filtercake weight per unit area applying the volume fractions of solid and fluid phases with their respective densities,

$$l(t) = \frac{W_{\text{wet filtercake}}(t)}{r_{\text{wet filtercake}}} = \frac{W_{\text{wet filtercake}}(t)}{f_{\text{f}}\, r_{\text{f}} + (1 - f_{\text{f}})\, r_{\text{l}}} \qquad \text{Eqn (8)}$$

where $W_{\text{wet filtercake}}(t)$ is the experimental weight of wet filtercake per unit area of the sample block, r_{l} is the density of the fluid phase and where, once again, f_{f} and r_{f} are the solids volume fraction and density of the dried filtercake respectively.

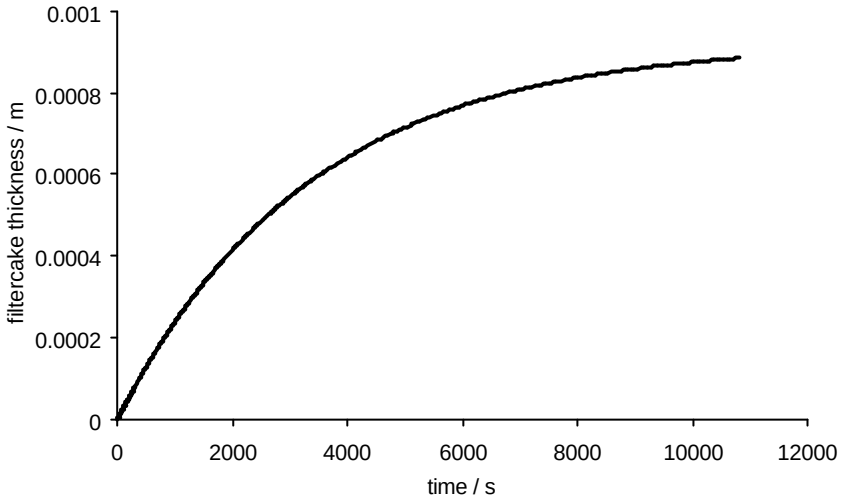

Figure 16 Progressive wet filtercake thickness as a function of time

Substituting $l(t)$ into equation 7 we obtain $K(t)$ as a description of the polymer capturing effect of the filtercake. As we see from Figure 17 there is a rapid change in $K(t)$ close to the start of the experiment. Physically, before the filtercake is established the effective *extra* permeability must be zero, i.e. $K(0) = 0$. Then as the filtercake begins to form and initially entangles polymers, it acts as a filter delivering fluid of lower polymer concentration to the substrate thus enhancing absorption rate. This short-lived increase in permeability occurs at about 100 s after the start of the experiment and can contribute up to a decade in increased permeability. After this initial maximum we can describe the equilibrating curve using an equation of the form,

$$K(t \geq 300) = a \tanh(b(t - c)) + d \qquad \text{Eqn (9)}$$

which is also shown in Figure 17, and obtain c = 1 500 seconds as the characteristic equlibrium absorbing lifetime of the porous substrate. The value of d (6.5×10^{-20} m^2) is a measure of the minimum permeability increase caused by the polymer capture effect in the equilibrium forming filtercake compared with the deposition from the free fluid phase that otherwise would be occurring in the porous substrate. Since this effect is relatively small it demonstrates that in flexographic printing the absorption of free reducer approximates to that of the fluid removal from the whole ink once this equilibrium is reached, i.e. it will be difficult to change the speed of absorption by adding reducer. Conversely, the effect of adding reducer is to lead to saturation of the coating. However, in the shorter timescale of real printing, the initial maximum permeability increase offered by the ink filter will have

a dominating effect. The value $1/b$ = 500 seconds is interpreted as the characteristic decay of absorption. This decay in absorption occurs once the filtercake and porous medium start to establish equilibrium as the polymer content in the filtercake increases in relation to the porous structural effects between the two media and the extent of the filtercake becomes large, i.e. as more polymer becomes filtered out and thereby concentrates in the extensive consolidating filtercake which increases the drag of the flow through the filtercake until the benefit from capturing the polymer is no longer seen. If we recall the structure recovery time of the ink after flow we see that this also was given by $\tau_0 \sim 550$ s which very closely matches this absorption decay parameter indicating the cessation of flow within the ink and its recovery after shear.

The definition of the asymptote at large t becomes uncertain as the equilibrium structure between the filtercake and the porous medium reduces the measurable flow and hence the differential in respect of hydraulic radii and this is well reflected in the scatter of the data points as the experiment proceeds. Once flow ceases, physically our overall permeability has no observable meaning even though it is inherent to the sample and since the evaluation depends on flow it is not possible to determine this intrinsic value. Our definition of $K(t)$ as an *added* permeability effected by the ink, however, should once again physically return to zero if it were measurable.

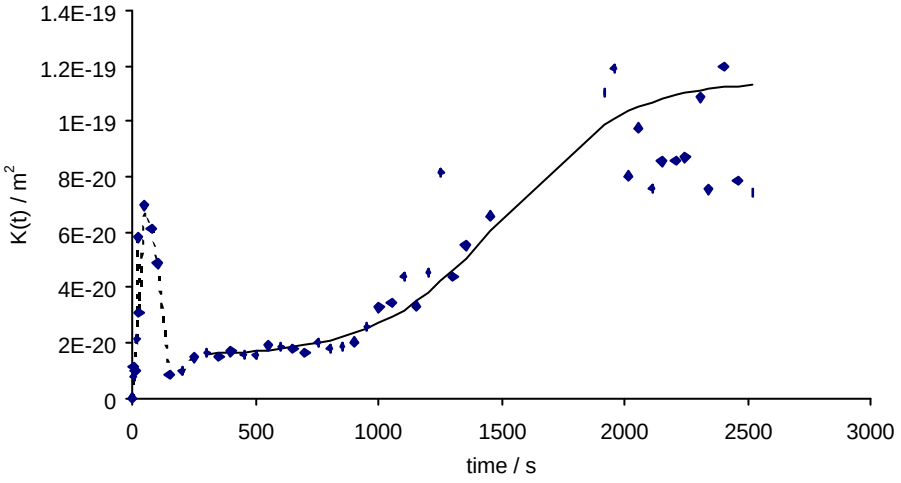

Figure 17 *K*(*t*) acting as a pump as a function of time, showing the polymer capture effect of the filtercake at shorter times and the relaxation of ink rheology as flow ceases toward the later stages of absorption

DISCUSSION AND PRACTICAL IMPLICATIONS IN PRINTING

Our model of the filtercake parameters uniquely include the effect of progressive polymer blocking of the absorbing structure. This factor is responsible for the time-dependent change of effective equivalent hydraulic radii and is not implicit in Darcy's equation. However, by maintaining the time

dependency, the Darcy relation is assumed to hold for all t and is used to describe the additional increased absorption or pumping action caused by the effective removal of the dissolved polymer from the absorbing fluid by the progressively forming ink filtercake. This removal is expressed as a differential adsorption of the polymer between the filtercake and the otherwise free fluid imbibition.

By regarding the pressure drop otherwise caused by polymer blocking of the entry pores to the absorbing substrate as an opposing reaction to the absorbing action of the sample block we always maintain a realistic filtercake which allows flow until equilibrium is reached. What appears to be counter intuitive is that the effect of the filtercake reduces as a function of time. This is because the flow rate through it decreases and not because the combined filtercake-substrate structure has a higher permeability as a function of time for constant flow rate, i.e. at equilibrium setting, the filtercake has a larger Darcy coefficient as the flow through it approaches zero. This physical requirement, independent of polymer effects, is a fundamental boundary condition of the problem, and calls into question the approximation of Xiang and Bousfied (1998) who assume that K is always small. However, many of the basic features are treated in a similar theoretical manner with the supporting experimental evidence provided here for the existence of a filtercake. The application in this current work, using experimental data for flexographic inks, provides for a universal improved self-consistent model.

The requirements for an absorbent coated medium for flexographic printing can now be understood more clearly in relation to the extender and reducer employed in a standard ink. The important role played by the polymer in the reducer in developing a further retardational aspect to the imbibition of the fluid phase severely limits the use of reducer to enhance the effects of mechanical pinholing (too fast ink drying before it can run together to form solid tone areas) and can, in turn, lead to feathering and fill-in. The need for high absorbency to allow the freedom of reducer addition, or tone control through extender, is therefore a prerequisite as the trend toward a polymer-blocked non-absorbent substrate during imbibition changes the nature of the substrate in an uncontrollable way. Using the experimental approach described, the design of suitable coating pigment formulations can be tested to establish the minimal rate of change of observed equivalent hydraulic radius (obtained from equation 5) during absorption of reducer whilst maintaining sufficient absorption force against the formation of the filtercake, which in turn can be studied directly by following the absorption from the whole ink. Maintaining this balance demands not only the right balance of porosity and pore size distribution but possibly also the need for high surface area pigments to allow for adsorption of imbibed polymer without blockage of the main network pathways if the addition of reducer is to act in respect of rate of absorption rather than saturation of the coating structure. In typical coating structures in use today, the rate of absorption from the whole ink is expected to be similar to that of the reducer.

This model and its associated experimental methods highlight the difference between flexographic full-tone multicolour printing and that of offset raster development. To print a format requiring colour to contact absorbent coating and preprinted areas simultaneously will depend on matching the absorbency

between dried ink/filtercake and the virgin coating to prevent blocking (smearing) on the preprinted areas. As we have seen, the absorbency of the dried ink implies some inter-polymer diffusion of fluid into otherwise polymer-filled voids. The design of the fluid phase to enhance such diffusive mechanisms is expected to require the use of surfactants and/or a contrasting range of molecular weight polymer additives. Maintaining this balance on the press with minimal changes in concentration is a constant challenge under the highly volatile conditions of the ink. The evaporation rates should therefore be fast enough to provide for anti-blocking but should not exceed the initial absorptive rate of the coating layer.

We have seen that the dried filtercake layer in contact with the coating surface approaches the theoretical maximum packing for sterically stabilised colloids. To enhance compatibility between coatings and preformed ink layers, the electrostatically stabilised coating pigments should ideally be controlled to develop similar packing strategies. Once again, since the packing characteristics are basically different between polymer stabilisation and electrostatic stabilisation (hard versus soft repulsion), chemical additives used in the coating or pigments of radically different morphology/surface area ratios could be an area for fruitful research.

CONCLUSIONS

Experimental absorption characteristics of flexographic inks have been studied by scaling the substrate dimensions to allow for supersource imbibition volumes. This avoids saturation of the coating layer before sufficient volumes of fluid can be absorbed to provide reproducible measurable results. The formation of compressed pigment blocks of coating grade ground calcium carbonate has provided the basis for the time-dependent observed absorption of fluid phase both from a complete flexographic ink and independently by centrifuging the ink to remove the ink solid phase. Analysis of the respective centrifuged fluid showed it to be essentially similar to that of its associated ink reducer. In contrast, the ink extender reported a similar chemical composition to that of the organic components in the ink.

Absorption of the free centrifuged fluid phase was seen to be additionally dependent on the dissolved polymer being carried into the absorbing structure. Account for this was made by retaining the time dependent variations of all parameters throughout the subsequent modelling of the absorption from the whole ink. Using a self-consistent pressure drop boundary condition applied to a filtercake model, the experimentally determined filtercake characteristics were applied to establish a characteristic Darcy coefficient as a function of time which formed a novel measure of differential polymer adsorption or retention in the immobilising ink. The pore-related parameters of the absorbing substrate and the filtercake, such as its solids volume fraction, porosity and elastic compressibility were determined using mercury porosimetry employing the correction for mercury compression, penetrometer expansion and, in the case of the absorbent, its skeletal compression. This description allowed for the effect of the filtercake on the absorption dynamic of a porous substrate to be analysed and was shown to be

progressive with time approaching equilibrium with the modified coating capillarity over a characteristic life time of absorption.

Acknowledgements

The authors wish to thank Mr. J. Schoelkopf of Omya, Plüss-Staufer AG for his assistance in the absorption experiment design and Dr. K. Ridgway (retired) for helpful discussions on determining layer mass distributions.

REFERENCES

Desjumaux, D., Bousfield, D. W., Glatter, T. P., Donigian, D. W., Ishley, J. N., Wise, K. J., (1998), "*Influence of Pigment Size on Wet Ink Gloss Development*", Journal of Pulp and Paper Science, 24, 150.

Finley, C., (1997), "*Printing Paper and Ink*", Delmar Publishers, New York.

Frith, W. J., Strivens, T. A., Mewis, J., (1990*), "Dynamic Mechanical-Properties of Polymerically Stabilized Dispersions*", Journal of Colloid and Interface Science, 139, 55.

Gane, P. A. C., Kettle, J. P., Matthews, G. P., Ridgway, C. J., (1995), "*Void Space Structure of Compressible Polymer Spheres and Consolidated Calcium Carbonate Paper-Coating Formulations*", Industrial and Engineering Chemistry Research, 35, 1753.

Gane, P. A. C., Schoelkopf, J., Spielmann, D. C., Matthews, G. P., Ridgway, C. J., (2000), "*Observing Fluid Transport into Porous Coating Structures: Some Novel Findings*", Tappi Journal, 85, 1.

Havlinova, B., Cicak, V., Brezova, V., Hornakova, L., (1999), "*Water-Reducible Flexographic Printing Inks - Rheological Behaviour and Interaction With Paper Substrates*", Journal of Materials Science, 34, 2081.

Macosko, C. W., (1994), "*Rheology: Principles, measurements and applications*", VCH Publishers, New York.

Moir, W.W., (1994), "Flexography - A Review", JOCCA-Surface Coatings International, 77, 221.

Schoelkopf, J., Gane, P. A. C., Ridgway, C. J., Matthews, G. P., (2000*), "Influence of Inertia on Liquid Absorption into Paper Coating Structures*", Nordic Pulp and Paper Research Journal, to be published.

Xiang,Y., Bousfield, D.W., (1998), "*The Influence of Coating Structure on Ink Tack Development*", PanPacific and International Printing and Graphic Arts Conference, CPPA, Canada, 93.